PNAS
www.pnas.org

Supplementary Information for

Pharmacological disruption of the Notch transcription factor complex

Rajwinder Lehal, Jelena Zaric, Michele Vigolo, Charlotte Urech, Viktoras Frismanatas, Nadine Zangger, Linlin Cao, Adeline Berger, Irene Chicote, Sylvain Loubéry, Sung Hee Choi, Ute Koch, Stephen C. Blacklow, Hector G. Palmer, Beat Bornhauser, Marcos Gonzalez-Gaitan, Yvan Arsenijevic, Vincent Zoete, Jon C. Aster, Jean-Pierre Bourquin, and Freddy Radtke

Corresponding author: Freddy Radtke
Email: Freddy.Radtke@epfl.ch

This PDF file includes:

Supplementary material and methods
Figures S1 to S15
SI References

www.pnas.org/cgi/doi/10.1073/pnas.1922606117

Supplementary material and methods

Cell lines and constructs

HeLa (#CCL-2) and HCC1187 (#CRL-2322) cell lines were obtained from the ATCC. TALL-1 (ACC-521) was obtained from DSMZ. RPMI-8402, KOPT-K1, DND-41 and HPB-ALL cell lines were a kind gift from Iannis Aifantis (NYU School of Medicine). Stable DL4-HeLa cells were generated using lentivirus particles expressing mouse DL4. Notch1-stable HeLa cells were created using pCDNA3.1-mNotch1-IRES-Puromycin vector. Notch responsive luciferase reporter was generated by cloning 12 x CSL binding sites [C(T)GTGGGAA] into pGL4.26.luciferase vector (Promega). SV40-Renilla vector was obtained from Promega. cDNA encoding the full-length human RBPJ gene was obtained from ORFeome Collaboration Collection and was cloned into pLEX-306 vector (Addgene) with an C-terminal V5- tag using Gateway technology (Thermo Fisher Scientific). The *RBPJ*^{G193R}, *RBPJ*^{L245A}, *RBPJ*^{L248A}, *RBPJ*^{F196A} and *RBPJ*^{G194R} point mutations were generated by Geneviz. Full length c-MYC cDNA was obtained from ORFeome Collaboration Collection and cloned into lentiviral vector pTRE-3xHA-IRES-GFP using Gateway technology (Thermo Fisher Scientific). DND-41 and DND-41-N1-ICD cells were transduced and sorted for GFP positive cells. MYC expression was validated by Western blot using the anti-HA-tag antibody. *N4-ICD* cDNA, a kind gift from Jon Aster (Brigham and Women's Hospital, Harvard Medical School), was cloned into lenti vector p4766 and driven by the human PGK promoter, using Gateway technology. The full length *NOTCH4* was obtained from ProteoGenix and cloned into lenti vector p4766, using Gateway technology. Oligos corresponding to sequence-paired sites with 16 base pairs spacers, oriented as head-to-tail or head-to-head (as previously described (1), as well as duplicates of each motives (as indicated in *SI Appendix* Fig. S5) were annealed and then cloned into pGL4.26.luciferase vector (Promega).

DL4:N1 co-culture screening assay

N1-HeLa cells were co-transfected with 12xCSL-luciferase and SV40-Renilla plasmids. DL4- and N1-HeLa cells were mixed in 1:1 ratio (5000:5000 cells/well) in 384 well assay plates (white, clear

bottom, Corning) using a Multidrop Combi reagent dispenser (Thermo Fisher Scientific). Chemical compound libraries assayed (NINDS II-Microsource Discovery Systems, HitFinder-Maybridge, PCL-Prestwick Chemical, KI Sellechkem, PPII Life Chemicals and Chemical Diverse Collection library provided by BSF, EPFL) were plated using a Biomek FX fluidic handler (Beckman Coulter) to give a final concentration 10 µM for a final assay volume of 22 µl. Twenty-four hours later, growth media was aspirated and cells were lysed with 1x Passive lysis buffer for 10 minutes at room temperature (RT). Luciferase activity was measured using Luciferase Assay Reagent II and Renilla values were determined by using Stop and Glow reagent (Dual luciferase assay system, Cat #E1980, Promega). Luciferase and Renilla readouts were taken using an Infinite F500 multimode reader (Tecan). All the liquid handling steps (aspiration of the medium, dispensing of Passive lysis buffer, Luciferase Assay Reagent II and Stop and Glow reagents were performed using an ELF406 washer-dispenser (BioTek). Data analyses were performed using in-house built analyses software at Biomolecular Screening Facility (BSF) at Ecole Polytechnique Fédérale de Lausanne (EPFL).

Luciferase reporter assay

HeLa cells, grown to 90% confluency, were transfected with the following plasmids, using the FuGene HD at 3:1 DNA ratio: pGL4-26-12CSL-Luc (2 µg/well) (or different pGL4.26. luciferase constructs with SPSs, as indicated in *SI Appendix* Figure S5), SV40-Renilla (0.1 µg/well) and vector expressing active form cDNA of one of the four human *NOTCH* receptors (0.82 µg/well). Twenty-four hours later the cells were collected and plated in 96-well-plates at 7 x 10^3 cells and treated with different inhibitors, as indicated in Figure legends, in 6 technical replicates. The following day the cells were lysed with Passive Lysis buffer and Luciferase/Renilla activities were read using Dual Luciferase Assay kit (Promega), according to the manufacturer`s protocol and Tecan Infinite F500 multimode reader.

Primary cell culture

Human hTERT immortalized primary bone marrow mesenchymal stroma cells (MSC; provided by D. Campana, St. Jude Children's Research Hospital, Memphis, TN) were cultured in RPMI 1640

medium supplemented with 10 % heat-inactivated fetal bovine serum, L-glutamine (2 mM), penicillin/streptomycin (P/S; 100 IU/ml) and hydrocortisone (1 µM). Xenografted human T-ALL cells were co-cultured on MSC in AIMV medium (Gibco Life Technologies, Carlsbad, CA) at a cell number ratio of 10:1 at 37°C, 5% CO_2.

Primary T-ALL cell viability assay

MSCs were seeded in 384-well plates at a concentration of 2,500 cells per well in 30 µL AIMV medium. After 24 hours, ALL cells were added at a concentration of 25,000 to 30,000 cells per well in 27.5 µL AIMV. CB-103 or DMSO as control was added after an additional 24 hours at five different concentrations (from 10 nM to 25 µM). Three days later, ALL cells were collected from co-cultures by scraping and stained with 7-AAD (BD Pharmingen, San Jose, CA). Cell viability (7-AAD negative population) was measured by flow cytometry (BD FACS Canto™ II, BD Biosciences) using counting beads (SPHERO Accu Count Blanc Particles, Spherotech Inc., Lake Forest, IL) for cell count normalization. Data were analyzed using FlowJo (version 10, TreeStar).

Proliferation assay

Proliferation assays were performed in 96-well plates to determine the growth kinetics of Notch inhibitor treated cells using the AlamarBlue reagent. Cells (5000 cells/well) were treated with DMSO or Notch inhibitors for different time intervals. Each treatment was carried out in 6 replicates. To determine the growth kinetics, 10 µl of AlamarBlue (Life Technologies) was added to each well and incubated for 4 hours followed by plate reading using an Infinite F500 multimode reader (Tecan).

Sensory Organ explant culture

Drosophila of genotype w^{1118}*; Neur-Gal4, UAS-mRFP-Pon /* + were used, enabling the visualisation of sensory organ cells by their specific expression of mRFP-Pon. Dissection, drug treatment and immuno-stainings were performed as described(2).

Intestinal organoid culture

Organoid cultures were established from total intestinal crypt preparations as described previously(3). Briefly, small intestines were scraped of villi and cut into 2-4 mm pieces. After several washings using PBS, crypts were incubated with 2 mM EDTA, followed by passing through 70μm cell strainer. The crypt enriched fraction was resuspended in Matrigel and plated into 48-well plates at 100-500 crypts/well. The Advanced DMEM/F12 medium (Invitrogen) with mouse EGF (50 ng/ml), mouse Noggin (100 ng/ml) and human R-Spondin (1 μg/ml) was changed every other day. After 7 days the crypts were large enough to be passaged. Two days after establishing the secondary organoid cultures small molecule inhibitors were added as indicated in Figure legends. The medium was changed every other day. At the end of the experiment organoids were either processed for tissue or RNA analyses. For histology the organoids were fixed for 10 min with 4% PFA and subsequently embedded in HistoGel (ThermoScientific) and paraffin. RNA was prepared from Matrigel free organoids using TriFast (PeqLab).

Quantitative Real Time PCR

RNA was extracted from cells using TriFast (PeqLab). Total RNA extracted from cells was used to synthesize cDNA by reverse transcription reaction. Reverse transcription was performed using SuperScript™ RT (Invitrogen). QRT-PCR was carried out using 7900 HT Fast Real-Time PCR system (Applied Biosystems). The data was normalized to HPRT as a house-keeping gene. The melting curves and Ct values were analyzed with SDS software (Applied Biosystems).

Primers sequences were as follows:

For human genes:

HES1	5'TGGAAATGACAGTGAAGCACC3'	5'GTTCATGCACTCGCTGAAGC 3'
MYC	5'CTTCTCTCCGTCCTCGGATTC3'	5'GAAGGTGATCCAGACTCTGACCTT3'
DTX1	5'AAGAAGTTCACCGCAAGAGGATT3'	5'CTAGGTAGCTAGCGTCCGGGTAG3'
NOTCH1	5'TCAGCGGGATCCACTGTGAG3'	5'ACACAGGCAGGTGAACGAGTT G3'
HPRT	5'TGACACTGGCAAAACAATGCA3'	5'GGTCCTTTTCACCAGCAAGCT3'
NOTCH3	5'GATGAGCTTGGGAAATCAGC3'	GGGTCTCCTCCTTGCTATCC

For mouse genes:

Hes1	5`CGGCATTCCAAGCTAGAGAAGG3`	5`GGTAGGTCATGGCGTTGATCTG3`
Hes3	5`CATCCAGACCAGCTCTCTACCT 3`	5`CAAGCAACCGCGACCTTCTCAC3`,
Hes5	5`CCGTCAGCTACCTGAAACACAG3`	5`GGTCAGGAACTG TACCGCCTC3`,
Olfm4	5`GCCACTTTCCAATTTCAC3`	5`GAGCCTCTTCTCATACAC3`
Atoh1	5`GCCTTGCCGGACTCGCTTCTC3`	5`TCTGTGCCATCATCGCTGTTAGGG3`

`

Antibodies

Following antibodies were used for WB, IP, ChIP, IF and FACS analyses: Anti-Val 1744 N1-ICD (2421S, Cell Signaling Technology), anti-NOTCH3 (5276, Cell Signaling Technology), anti-Notch1 (sc-69014, Santa Cruz), anti-CSL (sc-28713, Santa Cruz), anti-HES1 (sc-25392, Santa Cruz), anti-Myc (Abcam, ab32072), anti-Tubulin Sigma, T9026), anti-Actin (Sigma, A1978), anti-mouse CD4 (clone GK1.5, eBioscience), anti-mouse CD8 (clone YTS169.4), anti-mouse CD21 (clone 8C12, eBioscience), anti-mouse CD23 (clone B3B4, eBioscience), anti-mouse B220 (clone RA3-6B2, eBioscience), anti-mouse ESAM (clone 1G8, Biolegend), anti-mouse CD11c (clone N418, eBioscience), anti-mouse CD45 (Clone 30-F11, eBioscience), anti-human CD45 (Clone HI30, BioLegend) and anti-human CD7 (Clone HIB19, BioLegend), anti-HA-tag (901501, BioLegend), anti-Ki67 (M3060, amsbio), anti-Cyclin D1 (clone SP4-R, Ventana), anti-RBPJ (5313, Cell Signaling Technology), anti-V5-tag (V8012, Sigma), anti-Caspase 3 (9661, Cell Signaling Technology), anti-CD31 (RB-10333-P, NeoMarkers), anti-Ki67 (cb16667, abcam), anti-Lectin TRITC-conjugated antibody (L-5264, Sigma).

Immunofluorescence microscopy

To perform immunofluorescence staining, HeLa cells were grown on cover slips, washed with ice-cold PBS, fixed with 4 % PFA and permeabilized using 0.3 % Triton X-100. Subsequently cells were blocked for 20 minutes with 1 % BSA and incubated with appropriate primary antibodies for one hour at RT. Alexa Fluor-488 conjugated secondary antibodies were used to detect primary antibodies. Cells were counterstained with DAPI and mounted in fluorescent mounting media.

Fluorescent images were viewed and captured using Zeiss Axioplan microscope at Bioimaging and optics core facility at EPFL.

Western blot analyses

Cells were lysed in RIPA buffer (50 mM Tris.Cl, pH 7.5, 150 mM NaCl, 1 % Nonidet P-40, 0.5 % sodium deoxycholate and 0.1 % SDS) for 30 minutes at 4°C. The samples were run on 8 % or 10 % acrylamide gel in Tris-glycine electrophoresis buffer (25 mM Tris, 250 mM glycine, 0.1 % SDS). Following separation on the acrylamide gel, protein samples were transferred on to PVDF membrane (PEQ lab, catalog number 39-3010) using transfer buffer (39 mM glycine, 48 mM Tris, 0.037 % SDS and 20 % methanol).

For immunoblotting, membranes were incubated overnight with primary antibodies at 4°C followed by HRP-conjugated secondary antibodies for one hour at RT. Signal was detected with Pierce ECL substrate (Pierce, 32106).

Computational docking studies.

The prediction of the most probable position of CB-103 on the system formed by the NOTCH1 transcription complex and the *HES1* promoter DNA was achieved through molecular docking. Making the assumption that CB-103 acts by preventing the formation of a genuine NOTCH1 transcription complex, or by impairing the binding of this complex to DNA, several docking campaigns were performed. First, CB-103 was docked on the full Notch1 transcription complex / *HES1* promoter DNA system to determine a possible binding mode on the native structure. The latter is available in the Protein Databank(4), entry 3V79(5). In addition, several other dockings were performed, each one after removing one of the components of the system: CSL, MAML, the ANK or RAM domain of N1-ICD, or ultimately the *HES1* promoter. These dockings were performed to determine if the preferred binding mode of CB-103 occurs in a position where it could prevent the binding of one of the components of the system, thus impacting the activity of Notch transcription pathway. Docking runs were performed following a consensus procedure, using the Autodock Vina(6) and Attracting Cavities(7) software. This procedure is based on the assumption

that a binding mode found probable by these two docking programs, which use different sampling procedures and scoring functions, is more reliable than another solution preferred by only one software. All docking studies were performed with a search space encompassing the entire system. The exhaustivity parameter of Autodock Vina was set to 500 to increase the conformational sampling. For Attracting Cavities, the initial sampling of the ligand rotatable angles was performed using 60 degrees steps while the minimum number of atoms between the inner and outer spheres centered on potential attracting points was set to 60 for the selection of the latter. All other parameter of Autodock Vina and Attracting Cavities were set to their default values. The enzyme structure was kept rigid during the docking procedure.

Immunoprecipitation assay

RPMI-8402 cells were treated with CB-103 for 14 hours and proteins isolated by lysis buffer (Tris 20mM, NaCl 300 mM, 1 % NP-40, 10 % glycerol, 1 mM PMSF and 1 x protease inhibitor (Roche). Cell lysates (1 mg) were incubated with 50 µl of Anti-V5 Agarose Affinity Gel, Clone V5-10 (A7345, Sigma) for 2 hours at RT. After washing the beads with the lysis buffer 3 times, 15 min at RT, proteins were eluted with SDS-PAGE loading buffer by incubating at 99^{o} C for 10 minutes and analyzed by Western blot.

Chromatin immunoprecipitation assay

For ChIP 1 × 10^6 cells were used. Cells were first fixed with 2 mM DSG (Di(N-succinimidyl) glutarate, CAS: 79642-50-5) for 45 min at RT, washed 3 times with PBS and 1 mM PMSF and subsequently fixed in 1% formaldehyde (CAS: 50-00-0) for 15 min at RT. After incubating in 125 mM Glycine for 10 min at RT, cells were washed 3 times with PBS and 1 mM PMSF and lysed for 10 min at 4°C in Lysis buffer (ChIP Assay Kit, Cat No 17-295, Millipore). The assay was done according to the manufacturer`s protocol. (The DNA was sonicated for 10 cycles 30 sec on/off at 4°C). Antibodies used were N1-ICD and V5 tag antibodies, 2 µg / 10^6 cells. The precipitated DNA was analyzed by qPCR (see primer list).

ChIP primers:

DTX1 +30000 (CBS):	5`ACATGCCAGACAGCAGAACA3`	5`AACCTTCCAGACCCTGTGTG3`
HES1 TSS:	5`CGTGTCTCCTCCTCCCATT 3`	5`GAGAGGTAGACGGGGGATTC3`
Human NDME c1:	5`GAGGCCCCCATTCATTACCC3`	5`GCAGTTCTTCCTACGCTGGT3`
HES1 2200:	5'AGGTCACCCAGAGTCAGGAA3`	5'CCAGCGTCTTGTTTGATGTG3'
DTX1 1700:	5'TGTGAATGACATGGCAGAGG3'	5'TGAATCTCCTGCCAGTACC3'
human neg cont(+1M *MYC*):	5′AATGCTGGGCTTCCAAGGA3′	5′GACCTTGGTGACTGTTGAGGAAAC3′

SLAM-seq (thio(SH)-linked alkylation for the metabolic sequencing of RNA) preparation and sequencing

RPMI-8402 cells were treated with a final concentration of 1 μM CB-103 for 1 hour, 4 or 24 hours. Newly synthesized RNA was labeled for each indicated time span at a final concentration of 100 μM 4-thiouridine (4sU, Sigma #T4509) (8). Cells were pelleted and snap frozen. RNA extraction was performed using the RNeasy Plus Mini Kit (Qiagen #74134). Total RNA was subjected to alkylation by iodoacetamide (10 mM, Sigma #I1149) for 15 min and RNA was re-purified by ethanol precipitation. High RNA quality was validated by TapeStation 4200 (Agilent). Five hundred ng alkylated RNA was used as input for generating 3'-end mRNA sequencing libraries using a commercially available kit (QuantSeq 3′ mRNA-Seq Library Prep Kit FWD for Illumina, Lexogen #015.24). NGS libraries were analyzed by Fragment Analyzer (Agilent). Strand-specific library construction and Illumina NextSeq 500 sequencing of single-end 75 nt reads were performed at the Gene Expression Core Facility (EPFL).

The SLAM-seq data was deposited in the Gene Expression Omnibus database under accession numbers GSE148228. For reviewers: GEO accession GSE148228: https://www.ncbi.nlm.nih.gov/geo/query/acc.cgi?acc=GSE148228; Token: ***sjkjmoyujpenlkz***

Gene expression profiling of KOPT-K1 and HPB-ALL cells treated with CB-103 - Differential expression analysis

Gene expression was measured on Affymetrix chip HuGene-1_0-st-v1, raw data were normalized with rma (package oligo) and filtered to keep the probe set with maximum variance for each characterized gene. Differential expression was computed with limma and p-values were adjusted with Benjamini-Hochberg method(65). Genes with FDR < 0.05 were considered significantly regulated.

Pathway analysis

Significantly changed genes (FDR < 0.05) were selected and a Fisher test was used to select over-represented pathways from the mSigDB version 6.0 Hallmark collection. P-values were adjusted with Benjamini-Hochberg method(65) and a FDR cutoff of 0.05 was applied. Gene set enrichment analysis (GSEA) was computed on the ranked list of differentially expressed genes(66).

Bioinformatic analyses

The first 12 nucleotides were trimmed according to QuantSeq 3' mRNA-Seq library for Illumina FWD guidelines, Truseq adapters were also trimmed. To detect T>C conversion events from the RNA-seq data sets, reads were processed using SlamDunk v.0.2.4 (http://github.com/t-neumann/slamdunk) with slamdunk all command using parameters as described(8). Reads were first mapped to the human genome (GRCh38), read length was set to 75 (-rl option), trimming from 12 base pairs from the 5' end (-5 12 option), reporting up to 100 alignments per read (-n 100 option) and activating the multi-mapper retention strategy (-m option). Variants were called and filtered out with a variant fraction of 0.2 (-mv option) and default filtering for base-quality cutoff of ≥27 (-mbq option). Reads were filtered for having ≥1 T>C conversions (-c 1 option), remaining parameters were left to their defaults.

T>C conversion rates were computed for each 3' UTR as follows: 3' UTR annotations were obtained from biomaRt (version 2.38.0), mart ENSEMBL_MART_ENSEMBL (Ensembl Genes 96). Only the main chromosomes and protein coding transcripts were kept with UTRs annotated: a total of 56'975 annotated 3' UTR interval for 19'152 genes. For each T-position in a given 3' UTR, the

number of reads covering this position and the number of reads with T to C conversion at this position were recorded; both values were summed over all T-positions in the UTR, and the conversion rate for the UTR was computed as the percentage of reads with T>C conversion relative to the total number of reads.

For gene-level analysis, raw reads mapped to different UTR annotations of the same gene were summed up by gene. Size factors were estimated on total mRNA reads for global normalization with DESeq2 (version 1.26.0). Genes with average total mRNA reads ≥3.5 and average T>C converted reads ≥1.5 were kept (n=11'684) for differential expression with DESeq2. Genes with p-value < 0.05 and -1 < LFC < 1 were considered significant (Dataset S1). Gene Set Enrichment Analysis (GSEA)(9) was performed with mSigDB v7.0 collections Hallmark. p-value was obtained with 100'000 permutations and FDR adjusted (Dataset S2).

Flow cytometry analyses

Flow cytometric aquisition was performed on a Gallios cytometer (Beckman Coulter) or a BD FACS Canto™ II (BD Biosciences) at the Flow cytometry core facility, EPFL. MZB cell development was monitored using antibodies against B220, CD21 and CD23. $ESAM^+$ dendritic cells (DC) were identified using antibodies against CD11b, CD11c, CD8 and ESAM. Thymocytes were stained with antibodies directed against CD4 and CD8. Cell cycle analyses were performed using antibody against Ki67 and Hoechst dye. Flow cytometry analyses were done on live cells by gating on forward scatter (FSC) and side scatter (SSC) as previously described(10). Data were analyzed by FlowJo software (Tree Star, Ashland, OR).

Histology and immunostaining

Hematoxylin and eosin (H&E), Ki67 and cyclin D1 staining: Tissues were harvested, fixed in 4% paraformaldehyde (PFA) overnight at 4°C and embedded in paraffin. Tissue sections (4 microns) were stained with H&E. Cyclin D1 and Ki67 staining were performed using Ventana Roche Discovery XT system and revealed by DAB. Images were either captured using Leica DMI4000 microscope (2 x and 20 x objectives) or Olympus Slide Scanner VS120-L100 (40 x objective).

Alcian blue staining

Intestinal tissue was flushed with ice-cold PBS and fixed in 4 % PFA. Tissues were embedded in paraffin and sectioned to a thickness of 4 microns. Intestinal sections were deparaffinized, hydrated and Alcian blue staining was performed for 30 minutes at RT, washed in running water and finally counterstained in nuclear fast red solution for 5 minutes. Mounted sections were then viewed and images were captured using Olympus Slide Scanner VS120-L100 (40 x objective).

***In situ* hybridization**

The *in-situ* hybridization procedure using RNAscope HRP/DAB kit assay (Bio-techne, Cat. No. 323200) was performed on the fully automated Ventana Discovery ULTRA (Roche Diagnostics, Rotkreuz, Switzerland) platform according to manufacturer's protocol. All steps were performed on the machine with Ventana and Bio-techne solutions. 4 micron paraffin sections were hybridized with the negative control DapB (Bio-Techne, Cat. No. 312039) and positive control Mm-PPIB (Bio-Techne, Cat. No. 313919) probes as well as the target probes Mm-Atoh1 408799, Mm-Hes1 417709 and Mm-OLFM4 311839. Sections were counterstained with Mayer's hematoxylin and permanently mounted.

Retina flatmounts and staining

Enucleated eyes were fixed in 4 % PFA for 15 min, washed in PBS, followed by retina isolation as follows: cornea and lens were removed, four incisions were made in the neuronal tissue to detach it from the retinal pigment epithelium, choroid and sclera. The petal-shaped retina was fixed again in 4% paraformaldehyde for 30 min, washed in PBS and conserved for several days at 4° C. Retinas were then incubated into cold methanol (-20° C) for 10 min, washed in PBS and incubated in blocking solution (PBS, 0.1 % Triton, 3 % normal goat serum) for 1 hour at RT with gentle agitation. Tissues were then incubated in Lectin antibody solution (PBS, 0.1 % Triton, Sigma L-5264 TRITC-conjugated antibody diluted 1/100), overnight, at 4° C with gentle agitation, before to be flat-

mounted into mowiol. Z-stack of 6 steps each (total thickness of 4.9 µm and 2.3 µm at x20 and x40 magnification, respectively) were imaged using a DM6 B Leica microscope, treated by maximum intensity projection using the LAS X (Leica Application Suite X) software, and deconvolution with Huygens Essential software. Brightness intensity was homogeneously adjusted on Fiji software (Image J).

Compounds

6-[4-(tert-butyl)phenoxy]pyridin-3-amine (CB-103) and LY3039478 were purchased from SpiroChem (Switzerland**),** DAPT was purchased from Sigma (D5942) and RO4929097 from Roche. For intraperitoneal administration, the compounds were dissolved in corn oil by sonication. For oral administration, compounds were dissolved in 93 % water, 2 % Tween 80 and 5 % ethanol. In studies analysing the intestine (Fig. 4), splenic MZB (Fig. S10), T-cell development and $ESAM^+$ DC cells (Fig.S11) and retina (Fig. S12) mice (8-12 weeks) were treated twice daily for 7 days (intraperitoneal administration, 20mg/kg) or for 4 weeks in case of CB-103, only. Both CB-103 and LY3039478 were prepared fresh, daily, in 93% water, 5% ethanol and 2% Tween 80.

Tumor HCC-1187 xenograft assay

HCC-1187 TBNC cell line was transduced with lentivirus particles expressing luciferase. One million cells were subcutaneously transplanted into NOD/SCID$\gamma c^{-/-}$ mice. Tumor development was monitored by injecting luciferase substrate luciferin (Biosynth, L-8820) and imaged using IVIS Xenogen live imaging system. Once tumors were established on day 11 post-transplant, mice were grouped for vehicle (n=6) and CB-103 (n=6) treatment. Animals were treated with vehicle or CB-103 twice daily at 25mg/kg until day 30 post-transplant. Tumor volumes were measured at indicated time points.

Assessment of CB-103 activity on primary human T-ALL xenografts

Xenograft experiments were conducted with approval from the veterinary office of the Canton of Zürich. T-ALL cells were recovered from cryopreserved xenograft samples and 5 x 10^6 cells were

intravenously transplanted per mouse. Follow up of the circulating leukemia cells was performed every 7 days by flow cytometry after tail vein bleeding with anti-mouse CD45, anti-human CD45 and anti-human CD7. When the engraftment reached 10% human cells in the peripheral blood, randomized cohorts were treated with 10 or 25 mg/kg of CB-103 or vehicle control, with 3-4 mice per treatment arm. Follow-up was performed as before by flow cytometry after tail vein bleeding.

Statistical Analyses

Graphs and statistics were generated using GraphPad Prism 7 with default parameters. The significance of differences between groups was evaluated by using, unpaired *t*-test, one-, two-, or three-way analysis of variance (ANOVA). A *p*-value of <0.05 was considered statistically significant. The figure legends specify the method used and p-values. All cell-based experiments were performed at least three times in triplicates.

Ethics statement

All animal work was carried out in accordance with Swiss national guidelines. This study was reviewed and approved by the cantonal veterinary service, Vaud.

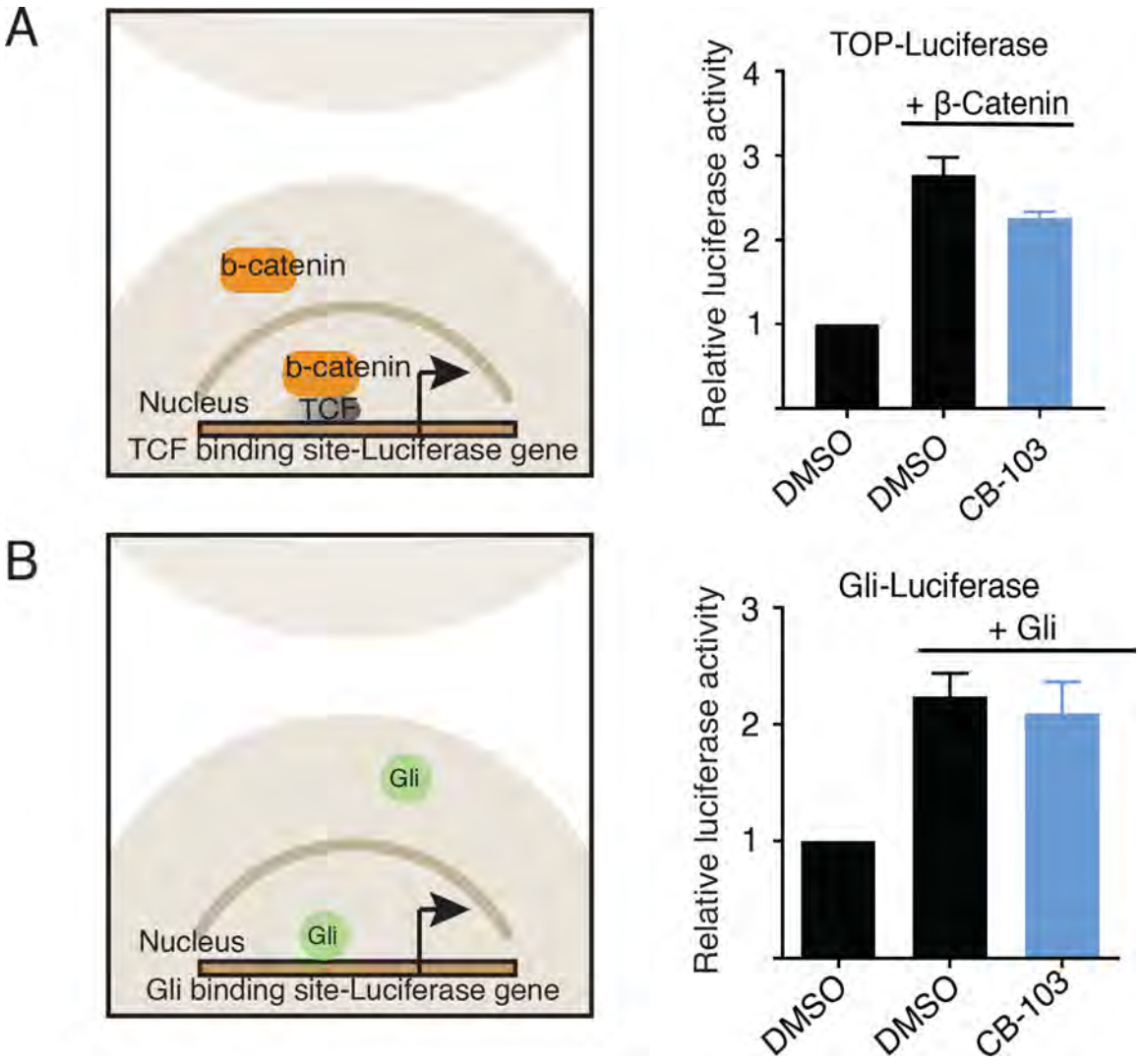

Fig. S1. CB-103 does not interfere with Wnt or Hedgehog signaling. (A and B) Left panels show schematic of TOP flash and Hedgehog signaling luciferase reporter assay while right panels show bar diagrams of reporter activity for canonical Wnt and Gli-mediated Hedgehog signaling in HeLa cells treated with DMSO and CB-103 (10 μM) for 24 hours (representative of two independent experiments with 8 replicates each).

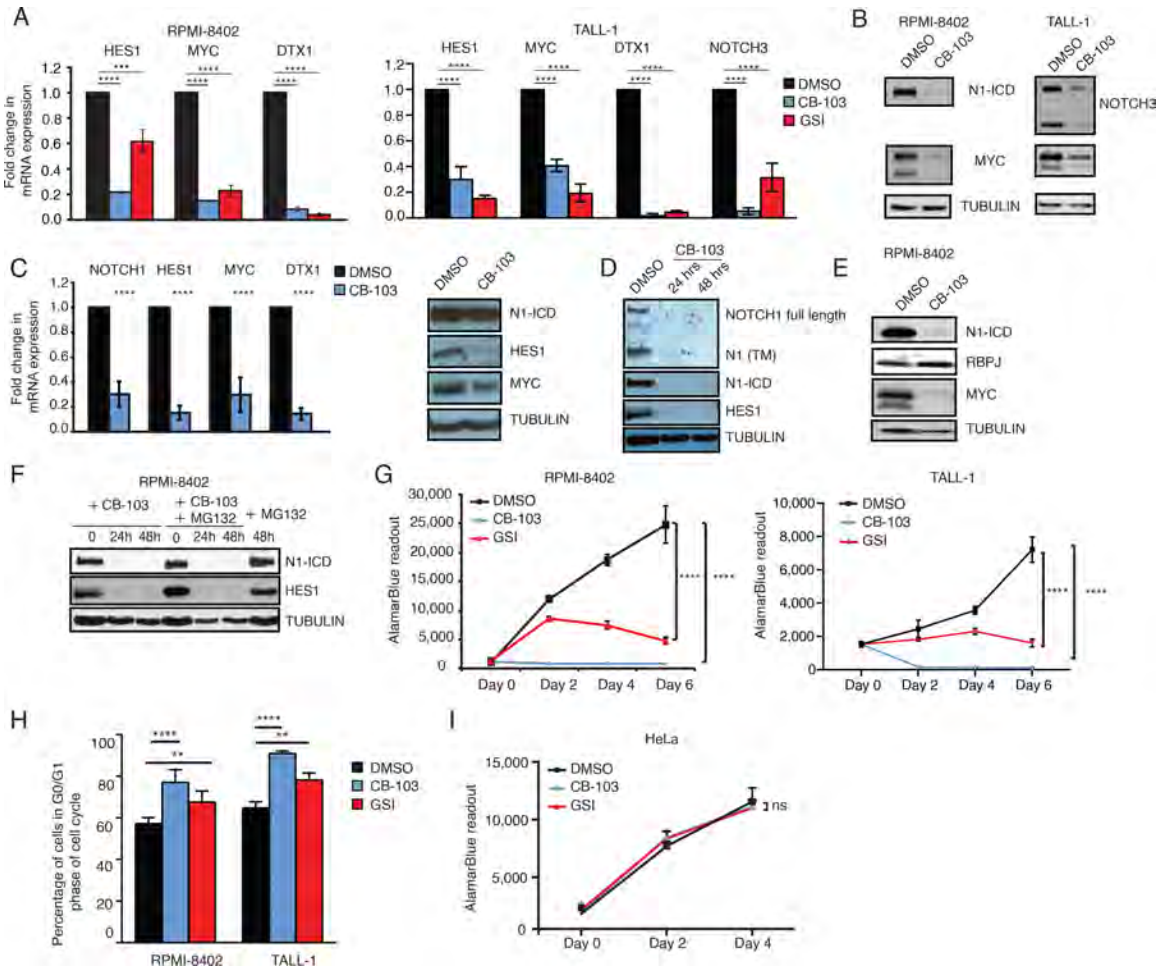

Fig. S2. Down regulation of Notch target genes and growth inhibition of CB-103-treated human Notch driven T-ALL cell lines. (A) Human T-ALL cell lines RPMI-8402 and TALL-1 were treated with DMSO, GSI (DAPT and LY3039478) and CB-103 (10 μM) for 24 hours. mRNA expression levels of NOTCH target genes *HES1*, *MYC* and *DTX1* were determined by qPCR and normalized to *HPRT*. Statistical analysis was performed using one-tailed t-test. (*** $p < 0.001$). (B) Western blot analyses for N1-ICD, NOTCH3 and MYC performed on DMSO and CB-103 treated (10 μM, 24 hours) RPMI-8402, and TALL-1 cells as indicated (representative Western blots of 5 independent experiments). (C) Bar graphs show relative *NOTCH1*, *HES1*, *MYC* and *DTX1* transcript levels in RPMI-8402 cells following 6 hours treatment with DMSO and CB-103 (10 μM). Western blot analysis at 6 hours post CB-103 treatment shows protein expression levels of N1-ICD, HES1 and MYC. (D) Western blot analysis for NOTCH1 (full length NOTCH1, transmembrane bound and N1-ICD) and HES1 on RPMI-8402 cells treated with DMSO or CB-103 (10 μM) for 24 and 48 hours. (E) Western blot analysis for N1-ICD, RBPJ and MYC on RPMI 8402 cells treated with DMSO or CB-103 (10 μM) for 24 hours. (F) Western blot analysis for N1-ICD and HES1 on RPMI-8402 cells treated with DMSO or CB-103 with or without the proteasomal inhibitor MG132

for 24 and 48 hours. Expression level of TUBULIN was used as a loading control (C-F). (G) Graphs show growth kinetics of RPMI-8402 and TALL-1 cell lines treated with either DMSO, CB-103 or GSI (DAPT and LY3039478, 10 μM) for 6 days. Statistical analysis was performed at time point day 6 using one-tailed t-test. (**** $p < 0.0001$) (H) Bars represent percentage of RPMI-8402 and TALL-1 cells in G_0/G_1 phase of the cell cycle 48 hours post treatment with either DMSO, GSI (RO4929097, 10 μM or LY3039478, 10 μM) and CB-103 (10 μM) (data average of 3 independent experiments, error bars ± S.D). (I) Graph shows growth kinetics of HeLa cells treated with either DMSO, GSI (DAPT, 100 μM) or CB-103 (100 μM) for 4 days, to show that CB-103 does not result in growth inhibition due to generic toxicity.

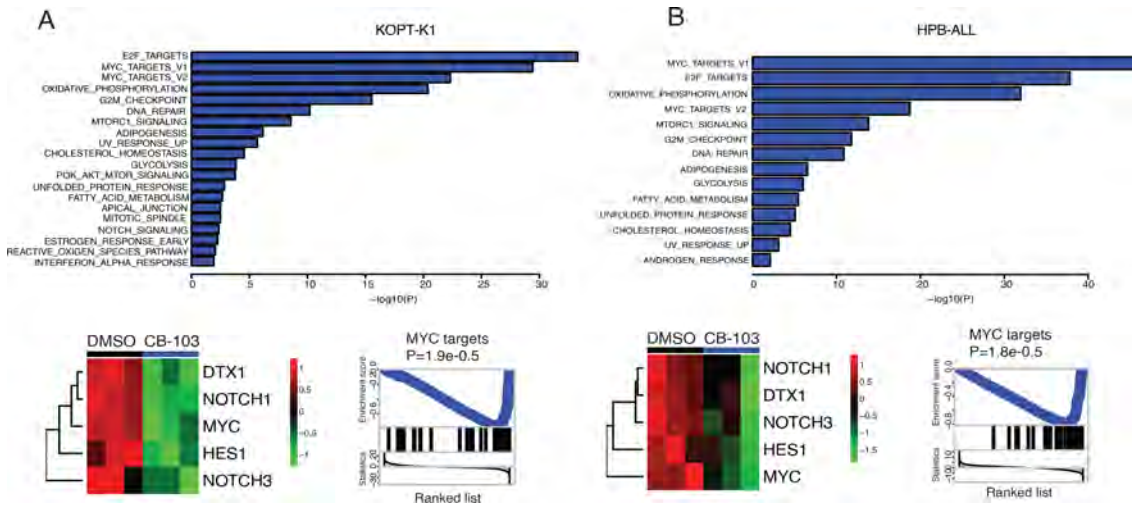

Fig. S3. Affymetrix gene expression analysis of CB-103 treated KOPT-K1 and HPB-ALL human T-ALL cell lines reveals down regulation of *NOTCH* and *MYC* target genes. Bar graphs show repressed Hallmark pathways (FDR < 0.05) and heat maps expression levels of *NOTCH* target genes in DMSO and CB-103 treated (24 hours at 10 μM) T-ALL cells. Gene Set Enrichment Analysis (GSEA) reveals *MYC* target gene downregulation (Hallmark collection from mSigDB) in genes ranked by differential expression between CB-103 and DMSO treated cells. (A) KOPT-K1 cells and (B) HPB-ALL cells.

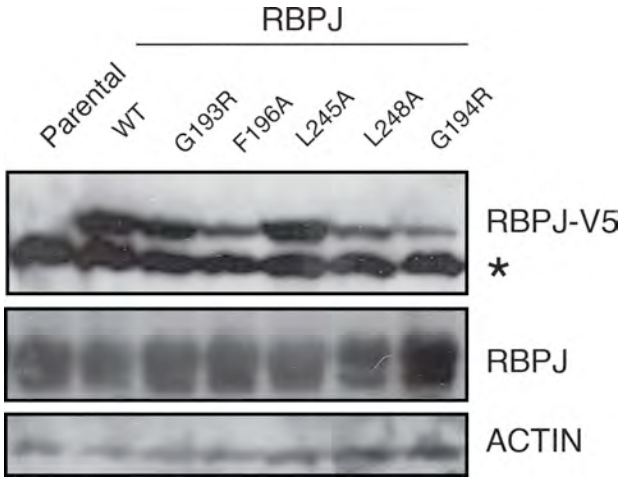

Fig. S4. Expression of RBPJ-mutants. Western blot probing for stable expression of RBPJ, RPBJ^{wt}–V5, RBPJ^{G193R}–V5, RBPJ^{G193R}–V5, RBPJ^{F196A}–V5, RBPJ^{L245A}–V5, RBPJ^{L248A}–V5, RBPJ^{G194R}–V5 in parental RPMI-8402 cells or those expressing WT or the mutant form of RBPJ using anti-V5-Tag or anti-RBPJ antibodies. Expression level of ACTIN was used as loading control. * indicates unspecific band.

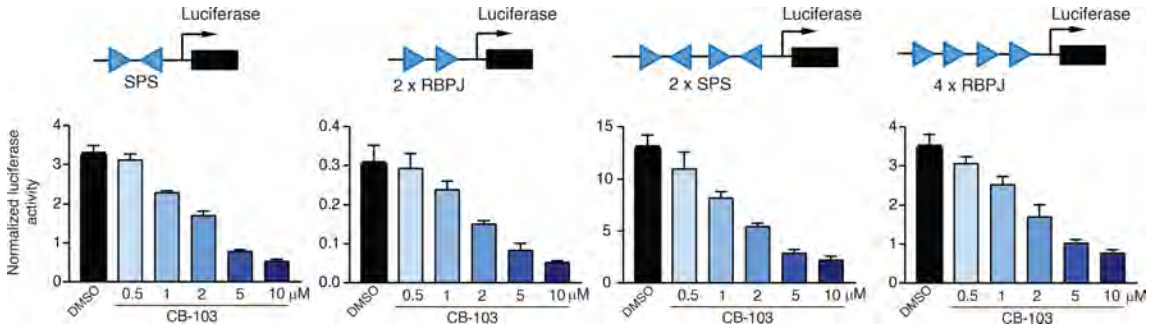

Fig. S5. Luciferase reporter analysis of head-to-tail and head-to-head oriented RBPJ binding sites. Upper panels show schematic representation of the RBPJ binding site-driven luciferase reporter constructs. Bar graphs show representative results of three individual experiments of N1-ICD induced luciferase activity in the presence of indicated concentrations (μM) of CB-103. For each concentration per reporter construct tested n=6.

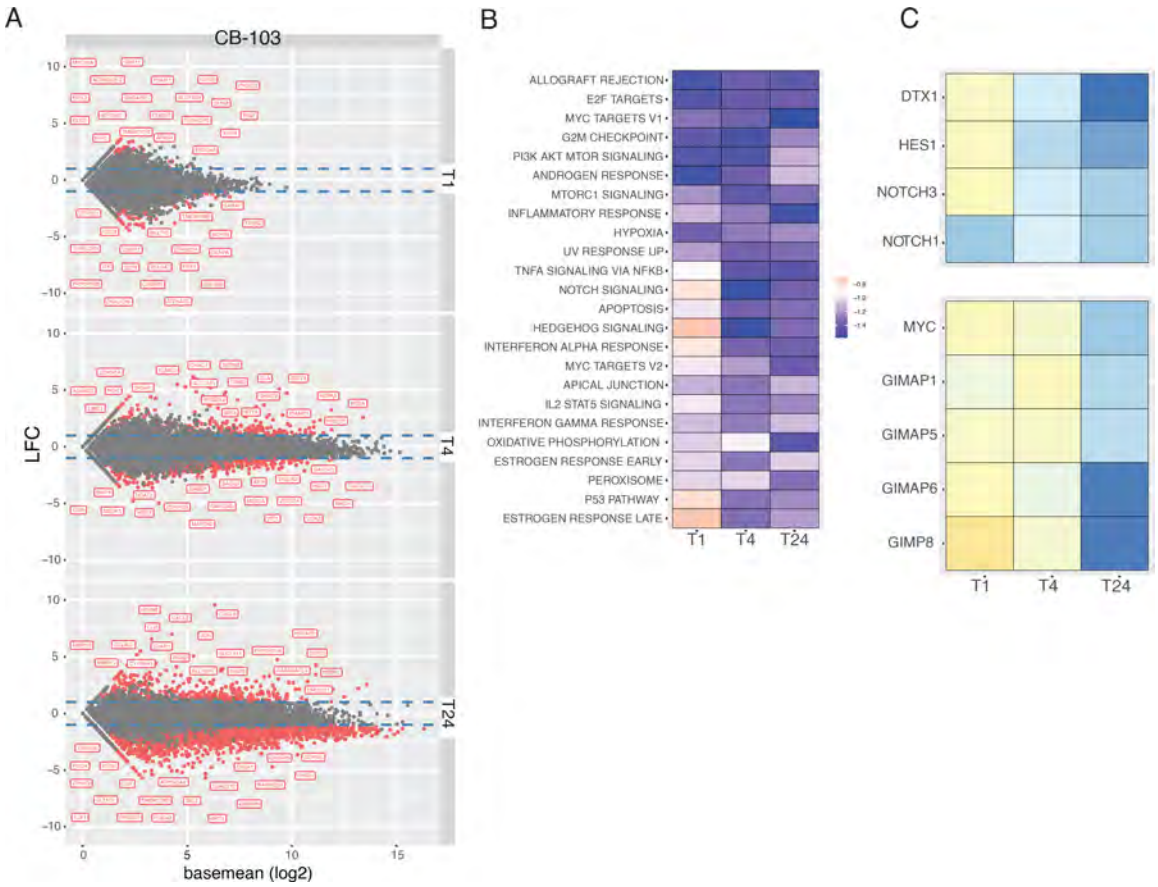

Fig. S6. SLAM-Seq analyses of CB-103 treated RPMI-8402 reveal different kinetics of target gene inhibition. (A) Newly synthesized RNA in RPMI-8402 cells treated with CB-103 for 1 hour (T1), 4 hours (T4) or 24 hours (T24). Red labels show the top 20 most induced and repressed genes with p-value < 0.05 and -1 < LFC <1. (B) Pathways from Hallmark collection (mSigDB) significantly repressed (FDR < 0.1) after treatment by CB-103 are depicted. Gene Set Enrichment Analysis (GSEA) was performed on ranked differentially expressed genes at three different time points 1 hour (T1), 4 hours (T4) or 24 hours post treatment with CB-103 compared to DMSO control. P-values were obtained by permutation test (n=100'000) and FDR adjusted (Benjamini & Hochberg). Color scale shows the normalized enrichment score (NES) obtained by GSEA. (C) Selection of Notch1 targets regulated at the promoter (top) or enhancer (bottom) level. Color scale shows LFC between 1 hour (T1), 4 hours (T4) or 24 hours (T24) post CB-103 treatment compared to 1 hour (T1), 4 hours (T4) or 24 hours (T24) DMSO-treated control (Red = induced, Yellow = unchanged, Blue = repressed).

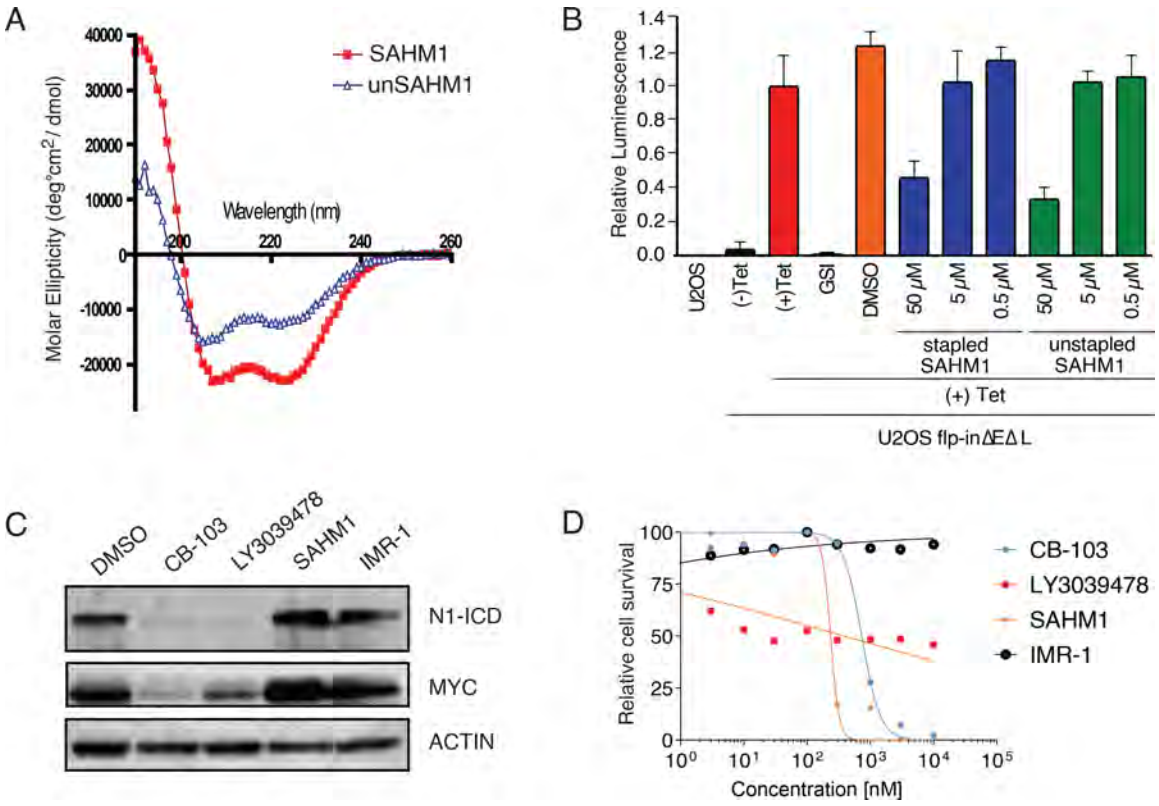

Fig. S7. CB-103 and LY3039478 but not SAHM1 or IMR-1 block Notch signaling. (A) CD spectra of SAHM1 and unstapled SAHM1 control peptide (unSAHM1). Spectra were acquired on a Jasco -815 CD Spectropolarimeter with a Peltier temperature controller and single cuvette holder. (B) Reporter gene assay. The potential inhibitory of SAHM1 and unstapled control peptide (unSAHM1) was tested in U2OS cells harboring a constitutively active form of Notch1 (ΔEΔL). Expression of ΔEΔL was induced and TP1 reporter activity was normalized to the activity of untreated control cells. The apparent IC50 of ~50 μM is an order of magnitude greater than previously claimed (32). (C) Western blot analysis for N1-ICD and MYC derived from RPMI-8402 T -ALL cells treated side by side with CB-103 (1 μM), LY3039478 (1 μM), SAHM1 (1 μM) and IMR-1 (1 μM). (D) Graph shows dose response curves of CB-103, LY3039478, SAHM1 and IMR-1 treated RPMI-8402 cells. Cells were treated with indicated compounds for 3 days.

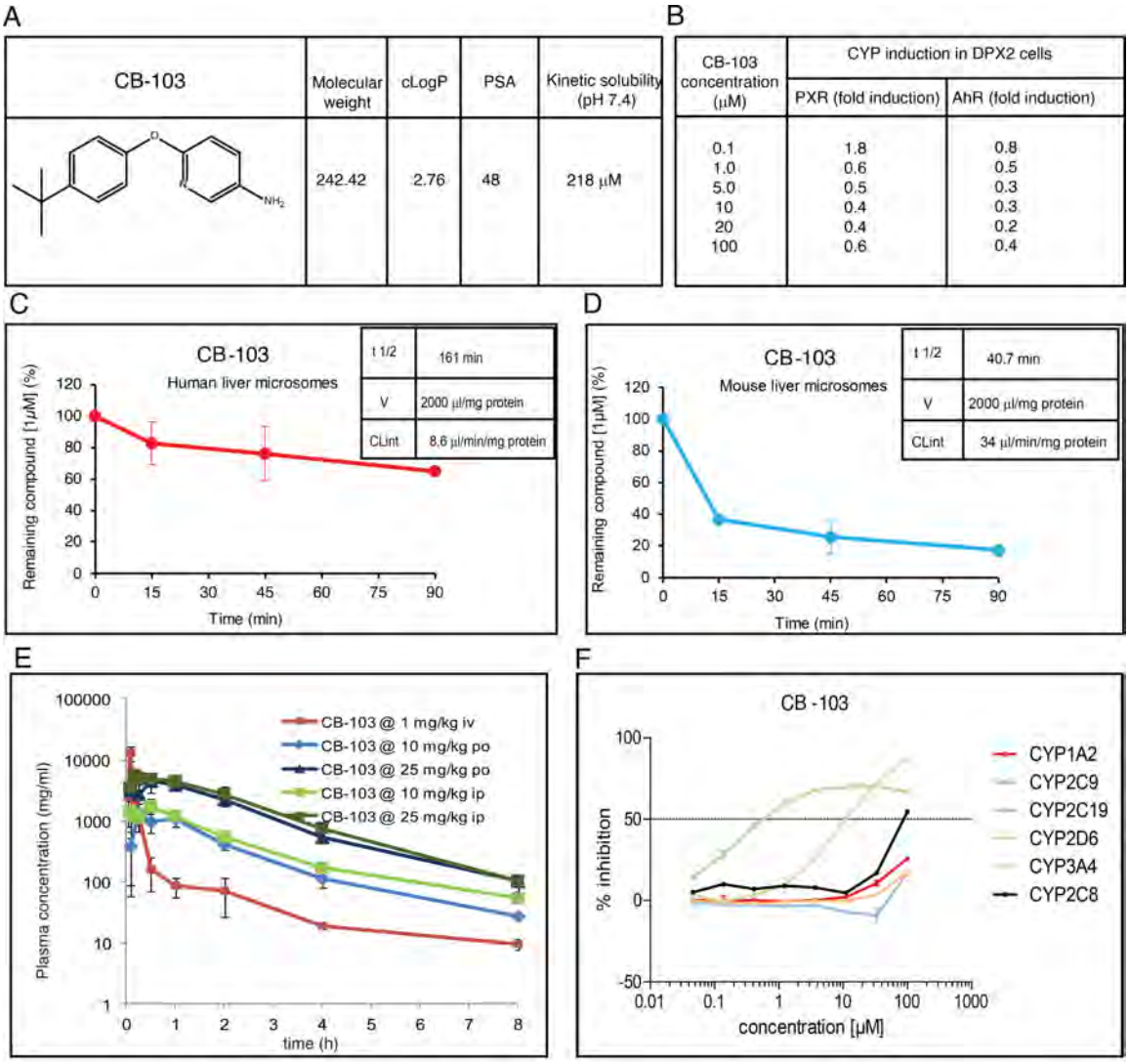

Fig. S8 CB-103 early ADME and Pharmakokinetic profiling. (A) Physiochemical properties of CB-103. With cLogP, PSA, and Kinetic solubility of 2.76, 48 and 218 µM respectively, CB-103 has the potential to cross lipid membranes, as well as the blood brain barrier, and has optimal solubility for appropriate formulation (B) CB-103 effect on CYP (Cytochrome P450) induction; (C-D) Half-life and clearance of CB-103 in human and mouse liver microsomes. (E) Pharmacokinetic profile of CB-103 in mouse. A comparison of CB-103 half-life in mouse and human liver microsomes indicates a shorter half-life in rodents compared to humans, which was further confirmed by pharmacokinetic analysis in mice. (F) CB-103 effect on CYP (Cytochrome P450) inhibition. (ADME – absorption, distribution, metabolism and excretion). One of the reasons for higher attrition rates of oncology drugs is their ability to inhibit or induce CYP enzymes. With the exception of minor

effects on CYP2C19, CB-103 does not significantly alter the activity any of the tested CYP enzymes as shown by CYP induction and inhibition assays

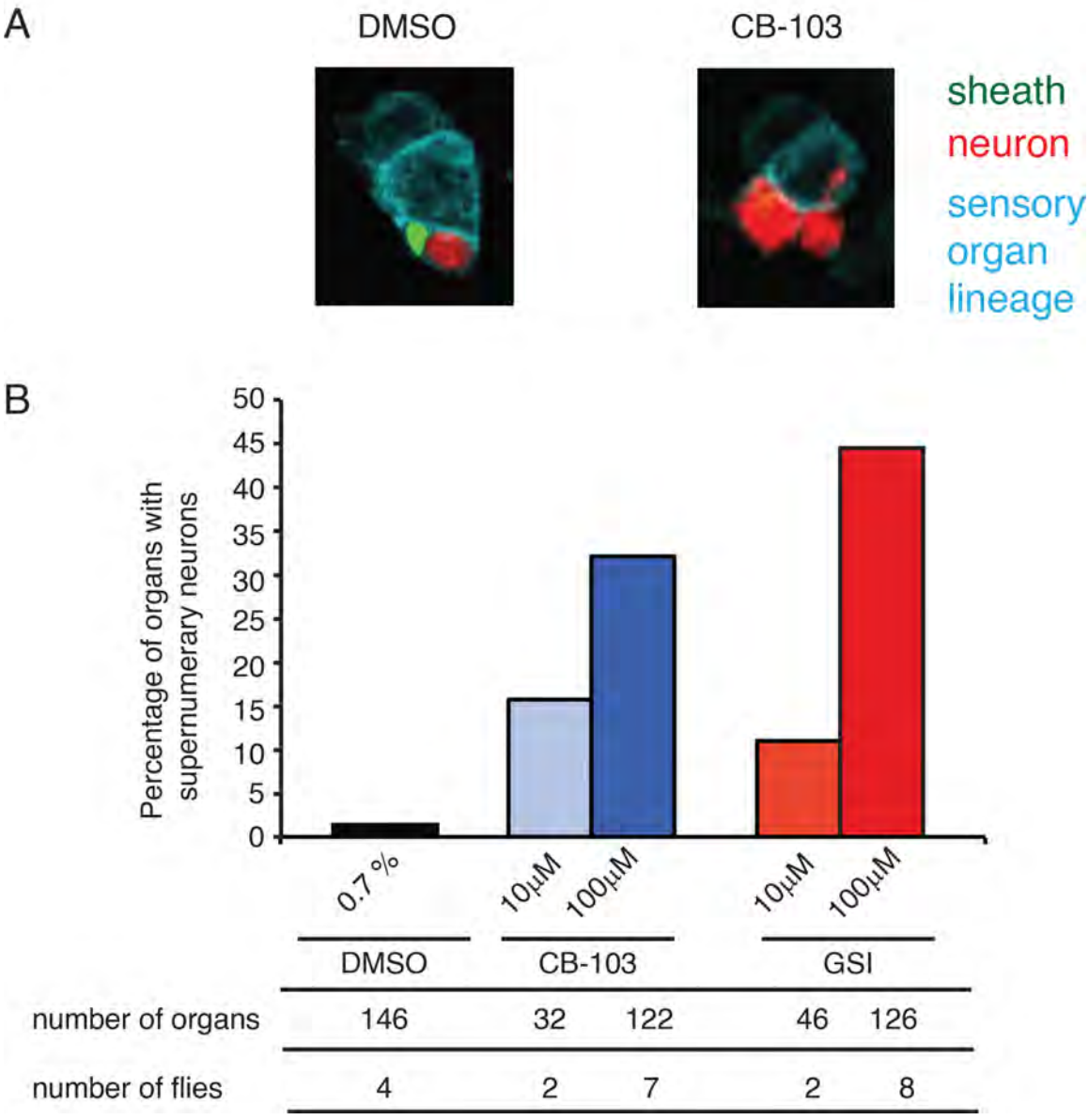

Fig. S9. CB-103 recapitulates Notch loss-of-function phenotypes in sensory organ explant culture of flies. Immuno-stainings in pupal nota for sheath cells (green) and neurons (red) reveal sensory organ lineages (cyan) with supernumerary neurons upon treatment with CB-103 or DAPT, Numbers of flies used and organs counted as indicated in the table.

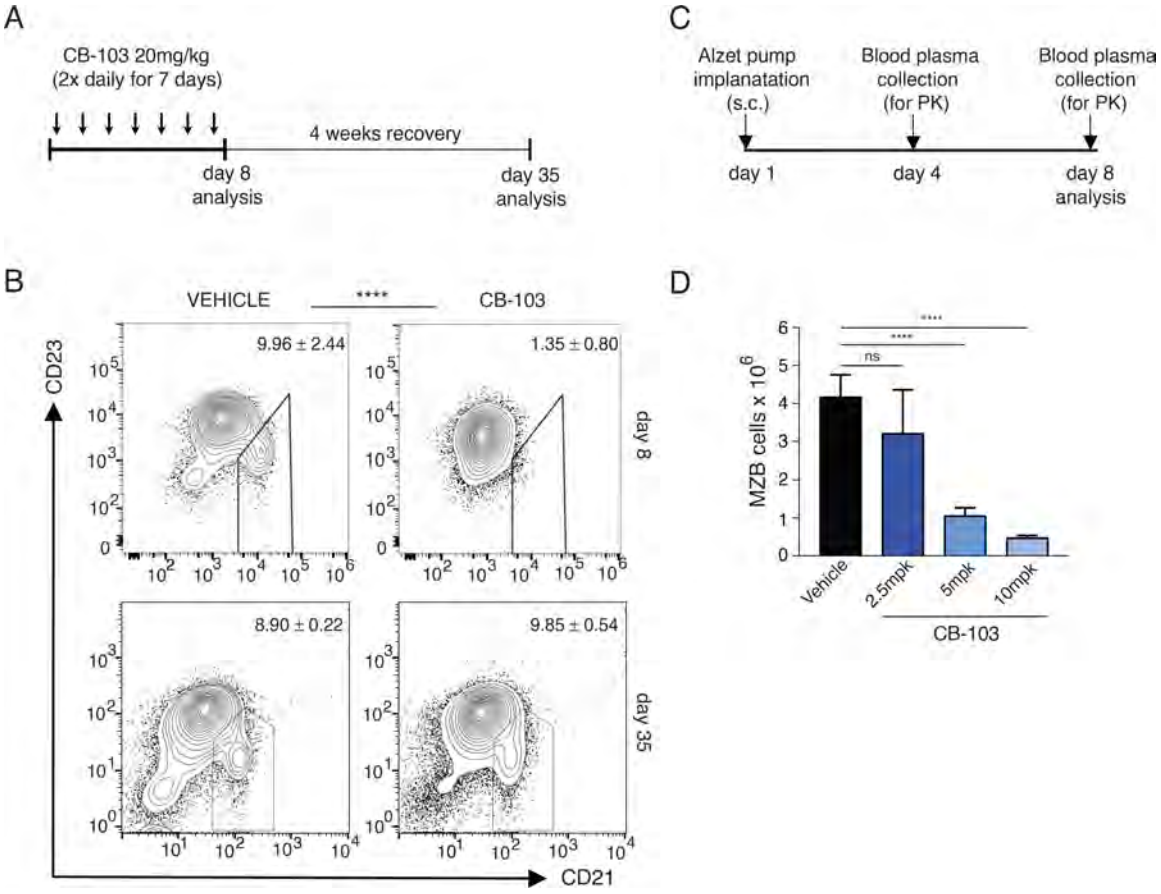

Fig. S10 CB-103 recapitulates Notch loss-of-function phenotypes *in vivo*. (A) Schematic representation of experimental set up. (B) Representative FACS profiles displaying the frequency of splenic MZB cells ($B220^{+}CD21^{hi}CD23^{int}$) in mice treated for 7 days (d) with either vehicle or CB-103 (25 mg/kg twice daily) prior to analyses on day 8 (n=3) or day 35 (B) after a 4-week recovery period (n=2). (C) Schematic representation of experimental set up. (D) Bar graphs show absolute numbers of MZB cells of mice carrying an osmotic pump to deliver sustained exposure levels of vehicle or CB-103 at indicated concentrations for 7 days prior analysis on day 8. (n=7 for vehicle control, n= 5 for 2.5 mpk, n=3 for 5 mpk, and n=3 for 10mpk; statistical analysis was performed using unpaired t-test **** $p < 0.0001$).

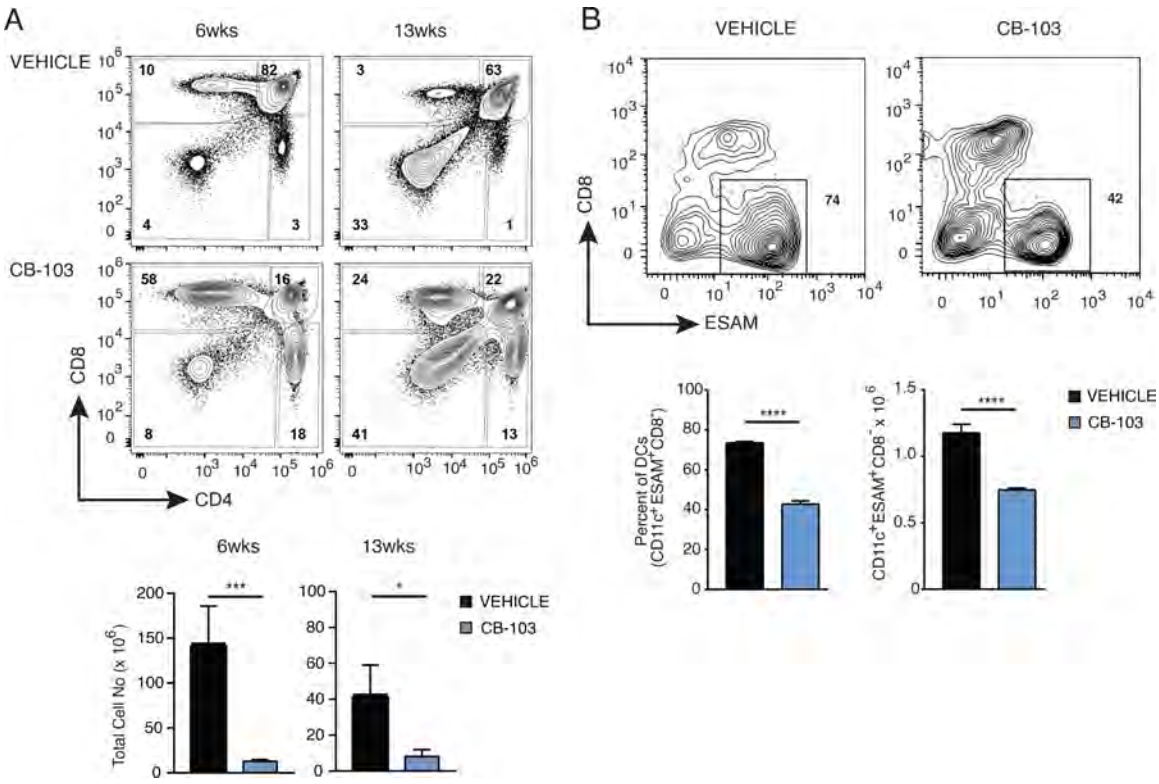

Fig. S11 CB-103 treatment impairs thymocyte and Esam+ splenic dendritic cell development. (A) Representative flow cytometric analysis of thymocytes derived from 6 and 13 week-old C57Bl/6 wt mice treated with either vehicle (n= 4 and n=6) or CB-103 (n= 3 and n=6) (20 mg/kg) for 7 days. For analysis at day 8, thymocytes were stained with anti-CD4 and anti-CD8 antibodies. Absolute cell numbers for total thymocytes are shown as bar diagrams, n=6 for vehicle treated and n=6 for CB-103 treated animals. (B) $ESAM^+$ splenic dendritic cells ($CD11c^+CD8^-B220^-$) in mice (n=6) treated with vehicle or CB-103 for 7days (25 mg/kg/day) prior to analyses on day 8.

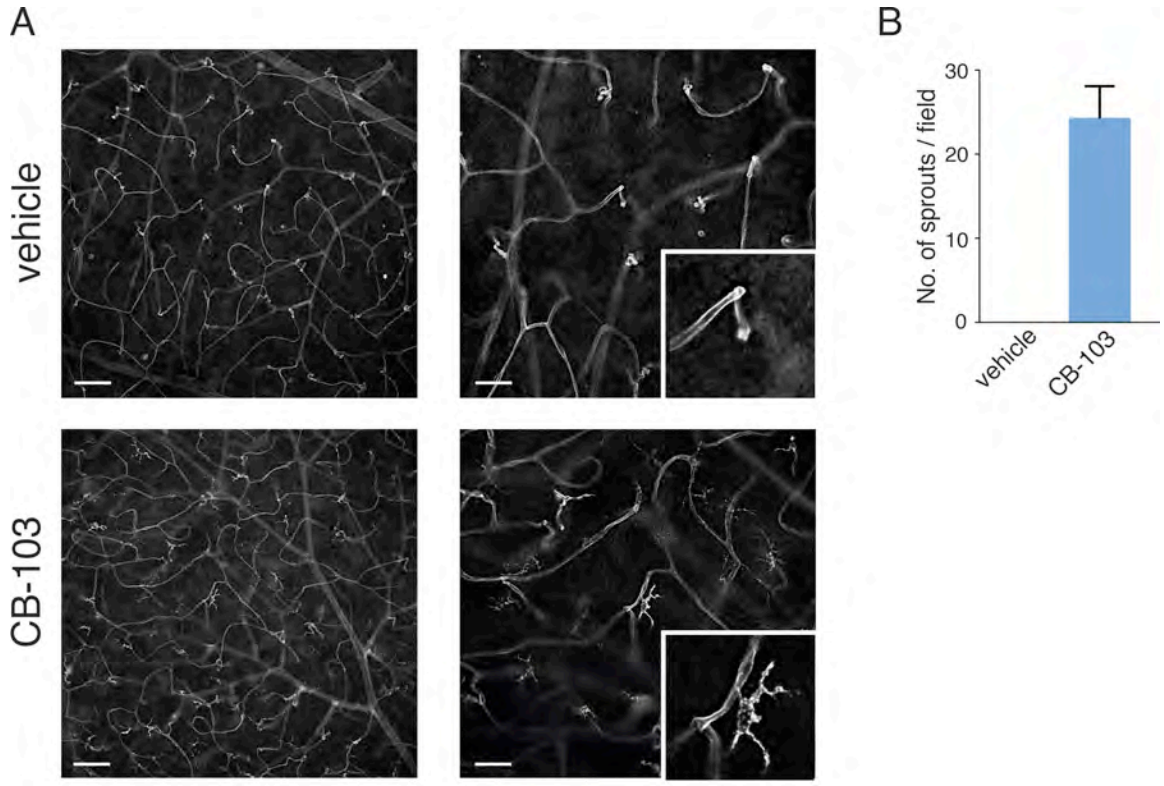

Fig. S12 CB-103 impacts on endothelial cell sprouting. (A) Retinal vasculature from 13 week-old adult mice treated with either vehicle or 20 mg/kg CB-103 for 7 days was visualized with lectin antibody. Images show representative retinal vasculature of vehicle (upper panels) (n=4) and CB-103 treated (n=6) lower panels, (left panels 20x, scale bar = 100 μm, right panels 40x scale bar = 50 μm, inset higher magnification taken from 40x panels). (B) Sprouting structures were counted in random images of superficial plexus at 20x, n=8 and expressed as average ± SD.

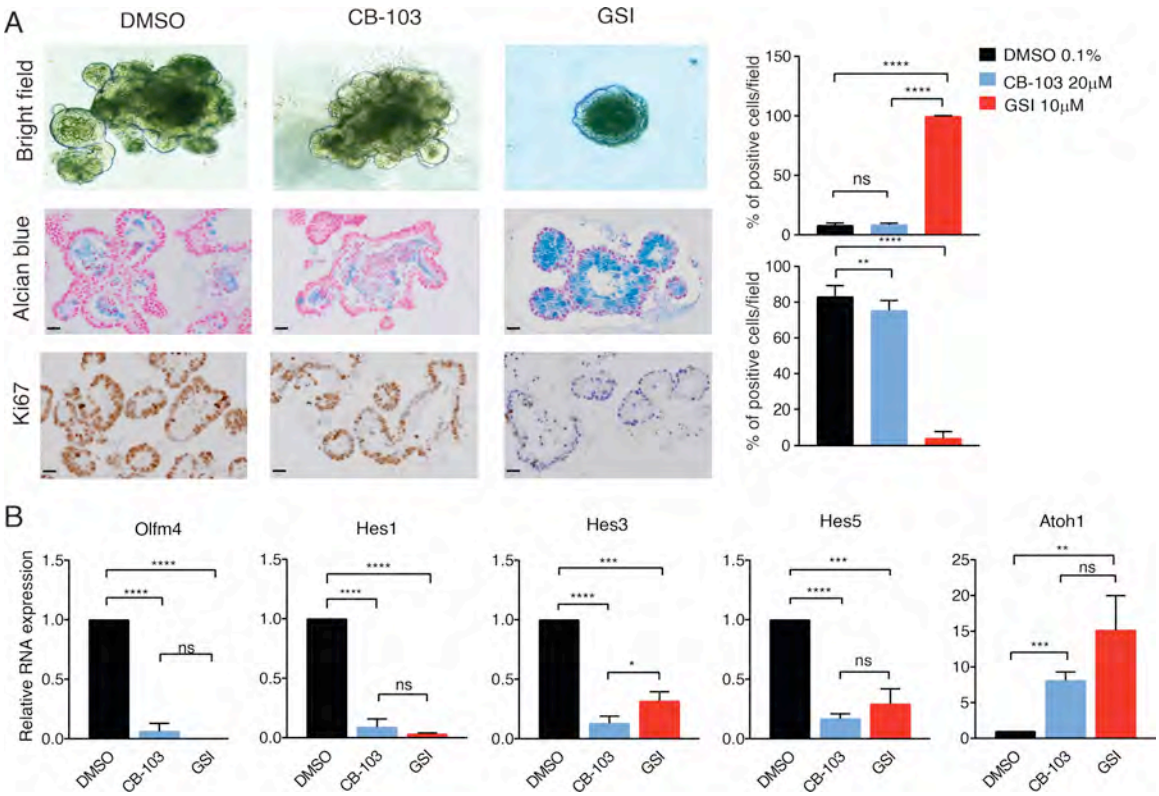

Fig. S13 CB-103 reduces *Notch* target gene expression in intestinal organoid cultures without causing goblet cell metaplasia. Intestinal organoid cultures were first established from wild type C57Bl/6 mice and subsequently treated with vehicle control (DMSO), CB-103 (20 μM) and LY3039478 (10 μM) for 5 days. (A) shows bright field images, Alcian blue and Ki67 staining of representative organoids, scale bar = 20 μm. Quantification of goblet cells and Ki67 positive cells are shown as relative percentage of Alcian blue^{+} and Ki67^{+} cells respectively to the right. (B) Bar graphs show relative mRNA expression levels for *Olmf4*, *Hes1*, *Hes3*, *Hes5* and *Atoh1* of vehicle, CB-103 (20 μM), and LY3039478 (10 μM) treated organoids. Data are representative of ≥ 3 independent experiments. Statistical analysis was performed using unpaired t-test. (**** $p < 0.0001$, ***$p < 0.0007$, ** $p < 0.008$, * $p < 0.03$).

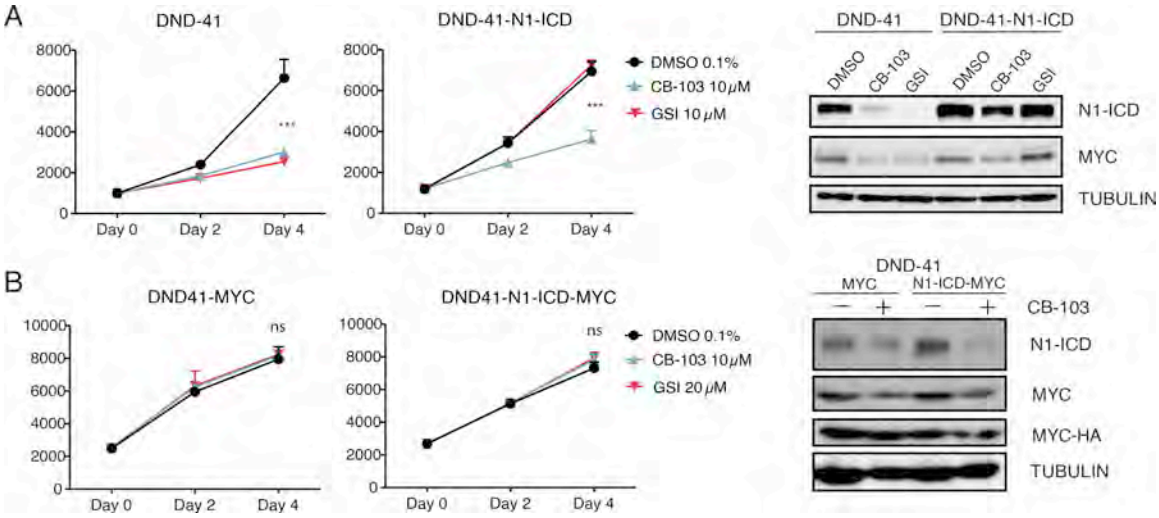

Fig. S14 Ectopic *MYC* expression rescues growth of CB-103 treated DND-41 T-ALL cells. (A) Growth kinetics of parental DND-41 and DND-41-N1-ICD cells treated with vehicle control, CB-103 (10 μM) and LY3039478 (10 μM) each for 4 days. CB-103 and LY3039478 inhibit growth of parental DND-41 cells, while DND-41 cells expressing N1-ICD is only inhibited by CB-103. Right panel shows Western blot analysis for N1-ICD and MYC on parental DND-41 and N1-ICD-transduced DND-41 cells treated with DMSO, CB-103 and LY3039478 (10 μM each). (B) Growth kinetics of parental DND-41 and DND-41-N1-ICD cells engineered to ectopically express *MYC* (DND41-MYC and DND-41-N1-ICD-MYC) treated with vehicle control and CB-103 (10 and 20 μM) each for 4 days. *MYC* expression rescues growth inhibition of CB-103 treated DND-41 cells. Right panel shows Western blot analysis for N1-ICD and MYC and HA-tagged MYC on DND-41-MYC and DND41-N1-ICD-MYC cells. Statistical analysis was performed using two-way ANOVA (*** $p < 0.0004$).

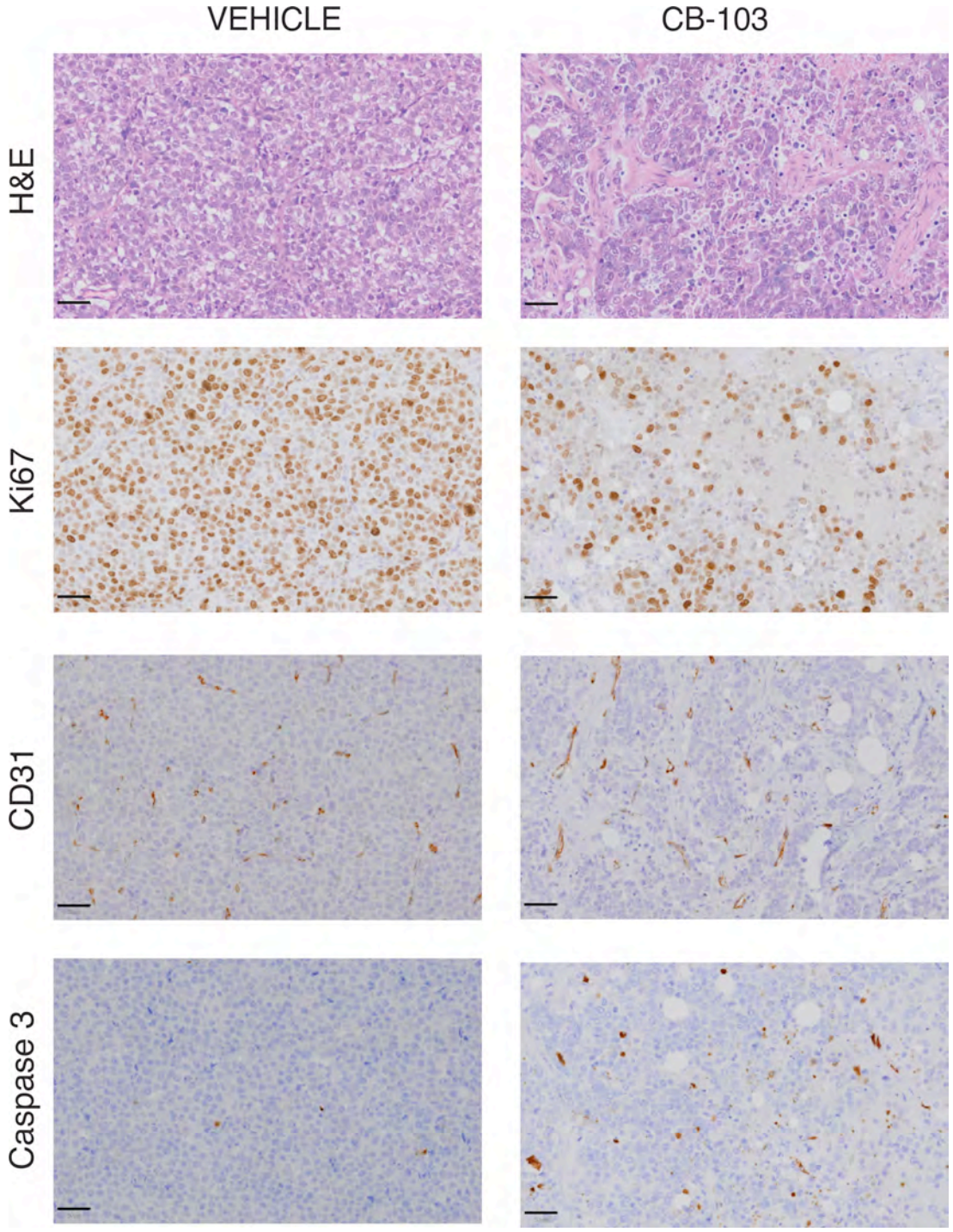

Fig. S15 Histological analysis of HCC-1187 xenotransplants. Panel shows representative hematoxylin and eosin staining and immunostaining for Ki67, CD31 and Caspase3 of HCC-1187-derived tumors harvested from vehicle n=6 and CB-103 treated NOD/SCIDγc$^{-/-}$ mice (n=6), treatment for 15 days (2 x/day), scale bar = 50 μm.

SI References

1. E. Severson, *et al.*, Genome-wide identification and characterization of Notch transcription complex–binding sequence-paired sites in leukemia cells. *Sci. Signal.* **10** (2017).

2. S. Loubéry, M. González-Gaitán, “Chapter Seventeen - Monitoring Notch/Delta Endosomal Trafficking and Signaling in Drosophila” in *Methods in Enzymology*, Endosome Signaling Part A., P. M. Conn, Ed. (Academic Press, 2014), pp. 301–321.

3. T. Sato, *et al.*, Single Lgr5 stem cells build crypt–villus structures *in vitro* without a mesenchymal niche. *Nature* **459**, 262–265 (2009).

4. D. R. Armstrong, *et al.*, PDBe: improved findability of macromolecular structure data in the PDB. *Nucleic Acids Res.* **48**, D335–D343 (2020).

5. S. H. Choi, *et al.*, Conformational Locking upon Cooperative Assembly of Notch Transcription Complexes. *Structure* **20**, 340–349 (2012).

6. O. Trott, A. J. Olson, AutoDock Vina: Improving the speed and accuracy of docking with a new scoring function, efficient optimization, and multithreading. *J. Comput. Chem.* **31**, 455–461 (2010).

7. V. Zoete, *et al.*, Attracting cavities for docking. Replacing the rough energy landscape of the protein by a smooth attracting landscape. *J. Comput. Chem.* **37**, 437–447 (2016).

8. M. Muhar, *et al.*, SLAM-seq defines direct gene-regulatory functions of the BRD4-MYC axis. *Science* **360**, 800–805 (2018).

9. A. Subramanian, *et al.*, Gene set enrichment analysis: A knowledge-based approach for interpreting genome-wide expression profiles. *Proc. Natl. Acad. Sci.* **102**, 15545–15550 (2005).

10. A. Wilson, H. R. MacDonald, F. Radtke, Notch 1–Deficient Common Lymphoid Precursors Adopt a B Cell Fate in the Thymus. *J. Exp. Med.* **194**, 1003–1012 (2001).